Prediction of Water Movement in Soil by Finite Element Method

Toshihiro MORII

(Received May 6, 1999)

ABSTRACT: A computer program SUSFEM for simulating water movement in two-dimensional or axisymmetric unsaturated, partially saturated, or saturated soil is developed. Richards' potential equation supplemented by appropriate boundary and initial conditions is described and formulated on the basis of Galerkin-type finite element method in conjunction with a fully implicit iterative scheme. SUSFEM calculates sequential and spatial variations of pressure head in soil, h. The saturated water movement is predominant in the region where $h>0$ and the unsaturated flow in the region where $h<0$. An equi-potential line corresponding to $h=0$ is defined as a free surface of seepage, a water table of groundwater, or a saturated water bulb of infiltration which happens to separate the saturated and unsaturated zones in the soil. Applicability of SUSFEM is examined fairly well by comparing with a laboratory experiment and a computer program published in the literatures. Then SUSFEM is applied to investigate a constant-head ifiltration from a single ring measured in sand soil field. It provides good predictions of the infiltration rate into the soil as well as the water movement in the soil with employing saturated hydraulic conductivity determined by field permeability test.

Key words: Water movement in soil, Richards' potential equation, Finite element method, Computer program, Field permeability test

INTRODUCTION

An importance of an accurate prediction of moisture movement in soil has long been recognized in various fields of technical science such as soil science and mechanics, water resources development, and agricultural and environmental engineering. Problems of the water movement in unsaturated and partly saturated soils lead to quasi-linear partial differential equations that are extremely difficult to solve by analytical methods. A numerical method based on a finite element method (FEM) is seemed to be the most effective tool to solve non-linear problems. Pioneering work toward development of the FEM analysis to investigate the moisture movement in soil has been done by NEUMAN[1]. In his study Richards' potential equation which integrates both the saturated and unsaturated water movements in soil is numerically solved by a Galerkin-type FEM in conjunction with a fully implicit iterative scheme. Perhaps one of the most excellent feature of saturated-unsaturated moisture movement analysis by using the FEM is an ability to treat almost all the boundary conditions such as precipitation, infiltration and evaporation from a soil surface, and water uptake by plant roots. Numerical solutions of the Richards' equation have been used, and likely will continue to be used in near future, for predicting the water movement in soil, and for analyzing specific laboratory or field experiments involving saturated and unsaturated water flow.

The purpose of the present work is to develop a computer program, SUSFEM, for simulating the water movement in two-dimensional unsaturated, partially saturated, or saturated soil. The Richards' potential equation is solved numerically using the Galerkin-type FEM, and a time derivative in the finite element equation is replaced by time-difference scheme. In the following an equation governing the water movement in soil is described and formulated. An applicability of SUSFEM is examined by comparing with a laboratory experiment and a computer program published in the literatures. Then SUSFEM is applied to analyze constant-head infiltration from a single ring into soil measured in sand soil field. The constant-head infiltration from the single ring forms theoretical base of a field permeability test using a

pressure infiltrometer method developed by REYNOLDS and ELRICK[2] and ELRICK and REYNOLDS[3]. The FEM analysis of the field measurement of the constant-head infiltration may provide practical information for applying the pressure infiltrometer method into the field soil.

GOVERNING EQUATION AND FINITE ELEMENT FORMULATION

Governing equation

The Richards' potential equation which integrates the saturated and unsaturated water flows in soil is given by[1]

$$\{K_r(h)K_{ij}{}^s h_{,j} + K_r(h)K_{i3}{}^s\}_{,i} = \left\{\frac{\theta(h)}{n} S_s + C_s(h)\right\}\frac{\partial h}{\partial t} \quad (i, j = 1, 2, 3) \tag{1}$$

where i and j are indices which represent horizontal coordinates x and y for $i, j=1$ and 2, respectively, and vertical coordinate z for $i, j=3$, t is time, $h=h(x, y, z, t)$ is a pressure head, $K_{ij}{}^s$ is a saturated hydraulic conductivity tensor, $K_r=K_r(h)$ is a relative hydraulic conductivity which is defined as a ratio of an unsaturated hydraulic conductivity divided by the saturated hydraulic conductivity of the soil ($0<K_r<1$), θ is a volumetric moisture content, n is a porosity, C_s is a specific moisture capacity defined as $\partial\theta/\partial h$, and S_s is a specific storage which is defined as volume of water instantaneously released from storage per unit bulk volume when h is lowered by one unit. Quantities with a single subscript and two subscripts in Eq. (1) represent components of vector and tensor variables, respectively. An index which appears twice in any given term of Eq. (1) follows summation convention. A comma in the equation means a partial differential by the index appearing after the comma. The functional relationships between θ, h and K_r are different for each soil and must be determined usually by laboratory or field experiments[4].

Eq. (1) should be supplemented by initial conditions

$$h(x, y, z, t) = h_0(x, y, z) \tag{2}$$

at each point in interior of a flow region. h_0 in Eq. (2) is a known value of the pressure head. In addition, either the pressure head or normal flux at each point along a boundary around the flow region must be specified as

$$h(x, y, z, t) = h_b(x, y, z, t) \quad on \quad \Gamma_1 \tag{3}$$

$$K_r(K_{ij}{}^s h_{,j} + K_{i3}{}^s)\, n_i = -v_b(x, y, z, t) \quad on \quad \Gamma_2 \tag{4}$$

where h_b is a known value of the pressure head prescribed on the boundary segment Γ_1, and v_b is a known value of the normal flux through the boundary Γ_2. n_i is a unit outer normal on Γ_2.

The solution $h=h(x, y, z, t)$ of Eq. (1) supplemented by Eqs. (2)-(4) describes sequential and spatial variations of the pressure head in the interior of the flow region. h is taken to be positive in the saturated zone and negative in the unsaturated zone. An equi-potential line or surface corresponding to $h=0$ gives a free surface in seepage problem, a water table in groundwater problem, or a saturated water bulb in infiltration problem.

Finite element formulation

By applying the Galerkin method in conjunction with a finite element discretization scheme, Eq. (1) subjected to Eqs. (2)-(4) is formulated into a set of quasi-linear first-order differential equation

$$A_{nm}h_m + F_{nm}\frac{\partial h_m}{\partial t} = Q_n - B_n \quad (n, m = 1, 2, \cdots, N) \tag{5}$$

where

$$A_{nm} = \sum_e \iint_{R^e} (K_{ij}{}^s K_{rl} \xi_l{}^e \xi_n{}^e{}_{,i} \xi_m{}^e{}_{,j})\, dR \tag{6a}$$

$$F_{nm} = \sum_e \delta_{nm} \iint_{R^e} \left(\frac{S_s}{n} \theta_l \xi_l{}^e + C_{sl} \xi_l{}^e\right) \xi_n{}^e dR \tag{6b}$$

$$Q_n = -\sum_e \oint_{\Gamma^e} (v_b{}^e \xi_n{}^e)\, d\Gamma \tag{6c}$$

$$B_n = \sum_e \iint_{R^e} (K_{i3}{}^s K_{rl} \xi_l{}^e \xi_n{}^e{}_{,i})\, dR \tag{6d}$$

Here n, m and l are dummy indices representing nodes in the flow region, N is a total number of the nodes, R^e and Γ^e are the interior and boundary of element e, and δ_{nm} is a Kronecker delta. Σ means a summation of the quantities along all the elements. ξ^e is a shape function specified according to the type of element employed in the finite element formulation.

Since the Galerkin method applies only at a given instant of time, the time derivative in Eq. (5) must be formulated independently and replaced by the time difference scheme as

$$\left[A_{nm} + \frac{\alpha}{\Delta t_k} F_{nm}\right]^{k+1/2} \{h_m\}^{k+1} = \alpha\{Q_n - B_n\}^{k+1/2} - \left[\beta A_{nm} - \frac{\alpha}{\Delta t_k} F_{nm}\right]^{k+1/2} \{h_m\}^k \quad (n, m = 1, 2, \cdots, N) \tag{7}$$

where k represents a time step and $\Delta t_k = t_{k+1} - t_k$ is a time increment at k. Parentheses $\{\cdot\}$ and $[\cdot]$ represent matrix and vector of the quantity, respectively. $\alpha = 2$ and $\beta = 1$ if time-centered time difference is adopted in Eq. (7), whereas $\alpha = 1$ and $\beta = 0$ for backward time difference. The time difference scheme should be selected according to the flow pattern in soil as well as the value of S_s as shown in Table 1.

The coefficients in Eq. (7) are evaluated at half the time step on the basis of $h^{k+1/2}$. A first estimate of $h^{k+1/2}$ can be obtained by linear extrapolation from h^{k-1} and h^k as

$$\{h_m\}^{k+1/2} = \{h_m\}^k + \frac{\Delta t_k}{2\Delta t_{k-1}} (\{h_m\}^k - \{h_m\}^{k-1}) \quad (m = 1, 2\cdots, N) \tag{8}$$

Eq. (7) is solved by a band matrix method using Gauss elimination for h^{k+1}. Since the unsaturated hydraulic properties of soil between θ, h and K_r are inherently nonlinear, h^{k+1} should be improved by iterative calculations. An improved estimate of the coefficients in Eq. (7) is done on the basis of updated $h^{k+1/2}$ given by

$$\{h_m\}^{k+1/2} = \frac{\{h_m\}^k + \{h_m\}^{k+1/2}}{2} \quad (m = 1, 2\cdots, N) \tag{9}$$

Table 1 The time difference scheme according to the flow pattern in soil and the value of S_s.

Specific storage S_s	Flow pattern		
	Unsaturated flow	Saturated-unsaturated flow	Saturated flow
$\neq 0$	-[a]	Time-centered	Time-centered
$=0$	Time-centerd	Backward	Direct solution[b]

a) S_s is always zero in the case of the unsaturated flow.

b) The governing equation reduces to a Laplace equation because the time derivative vanishes, which can be solved directly by the inverse of the matrix equation.

where the first term in the right-hand side is the pressure head calculated in the preceding time step k and the second term is the pressure head calculated in the preceding iterative calculation. The iterative calculation will be terminated if maximum difference between h^{k+1} just calculated and h^{k+1} calculated in the preceding iteration at each nodes becomes less than allowable tolerance, and the pressure head at the next time step will be calculated by Eq. (7) with the first estimate of $h^{k+1/2}$ given by Eq. (8).

Examination of applicability

To examine the applicability of SUSFEM, the numerical results will be compared with the laboratory experiment and the computer program published in the literatures.

VAUCLIN, et al.[5] investigated response of the water table to surface irrigation in the laboratory. Fig. 1 shows the laboratory setup employing a soil slab 300 cm long, 200 cm high and 5 cm thick. A fine river sand was compacted to construct the soil slab. The isotropic saturated hydraulic conductivity $K_{ij}{}^{s}=K_s$ and the porosity of the compacted soil are 35 cm/h and 0.3, respectively. S_s is assumed to be zero. Left-hand side of vertical ends of the soil slab was connected to a constant head reservoir. No flow was allowed through the other side of the vertical ends of the soil slab. The water table in the reservoir was set initially at a depth 65 cm above an impervious base of the soil slab. After hydrostatic equilibrium had been attained in the entire region of the soil slab, a constant flux q_0 corresponding to 14.8 cm/h was applied over a width 50 cm of the soil surface during eight hours. There was no surface runoff because $q_0 < K_s$. The unsaturated hydraulic properties of the sand soil was estimated on the basis of the measurements of the soil slab experiments as

$$\theta = \theta_s \frac{A}{A + |h|^B} \tag{10}$$

$$K = K_s \frac{C}{C + |h|^D} \tag{11}$$

where $\theta_s=0.03\ \mathrm{cm^3/cm^3}$, $A=40000$, $B=2.90$, $C=2.99\times10^6$ and $D=5.0$.

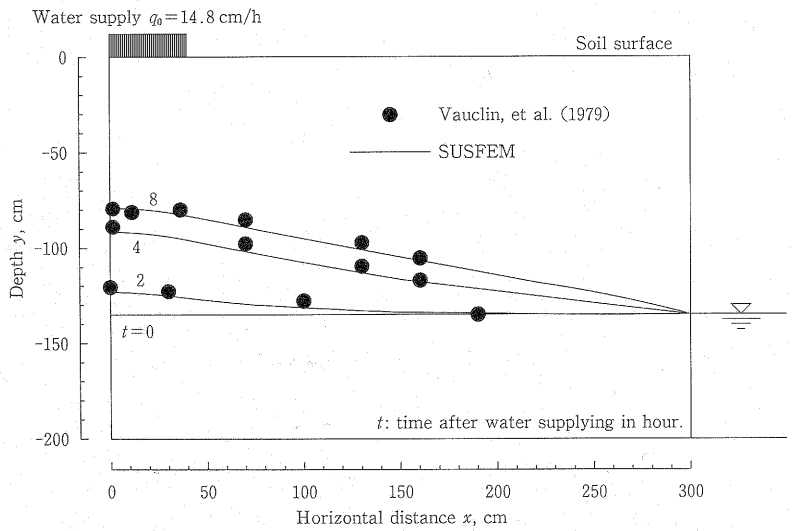

Fig. 1 Experimental setup using the soil slab conducted by VAUCLIN, et al.[5], and comparison of the water table calculated by SUSFEM with the experimental measurements.

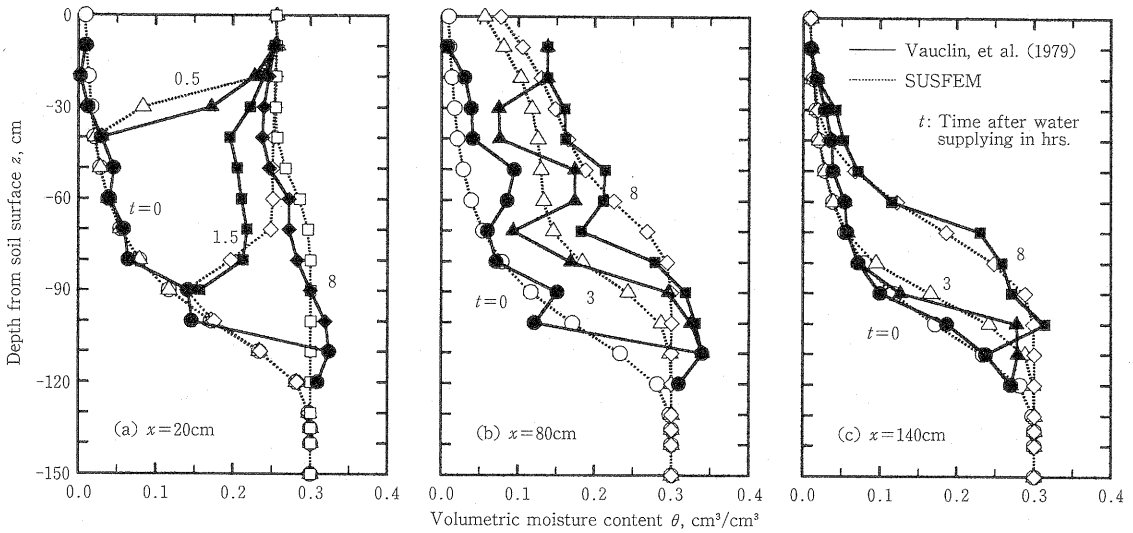

Fig. 2 Moisture profiles in the soil calculated by SUSFEM at $x=20$, 80 and 140 cm from the side end of the soil slab for different time compared with the experimental measurements conducted by VAUCLIN, et al.[5] The moisture profile at $t=0$ gives initial distribution of moisture content in the soil.

The water tables at different time calculated by SUSFEM are compared well with the experimental measurements as shown in Fig. 1. No flow is allowed through the base and the left-hand side vertibcal end of the soil slab and through the soil surface except for the infiltration zone. The vertical side of the soil slab above the constant water level is considered as a boundary segment along which a seepage face has a chance to develop during any stage of the calculations. The allowable tolerance of the pressure head to judge the convergence of the iterative calculations is set to be 0.01 cm. In Fig. 2, moisture profiles in the soil for different abscissa at $x=20$, 80 and 140 cm from the left-hand side end of the soil slab and for different time are compared between SUSFEM and the experimental measurements. The moisture profiles at $t=0$ are initial ones. Some irregular plots in the measurements may be responsible for local heterogeneity caused during the compaction of the sand soil. Fairly good agreement between SUSFEM and the experimental measurements can be seen in Fig. 2. It is noticed that the water movement below the infiltration zone is mostly vertical downward as shown in Fig. 2 (a), the water moves mostly in a horizontal direction at the region middle of the soil slab in Fig. 2 (b), and the water movement is predominantly upward in the region most apart from the infiltration zone as shown in Fig. 2 (c).

The computer program SWMS_2D is selected for the second examination of the applicability of SUSFEM. SWMS_2D has been developed by SIMUNEK, et al.[6] to investigate water and solute movements in two-dimensional variably saturated media. Axisymmetric water movement into soil from a infiltrometer placed on the soil surface is simulated both by SUSFEM and SWMS_2D. Fig. 3 shows a flow system together with the finite element mesh and the initial pressure head employed in the simulations. Two layered soil profile is considered. The saturated and unsaturated hydraulic properties of the soils are listed in Table 2. The unsaturated hydraulic properties of the soils are described by a functional model of van GENUCHTEN[7]. Numerical simulations are carried out over a period of 5 days. All sides of the flow region are assumed to be impervious except for the soil surface inside the infiltrometer 17 cm in radius. A constant pressure head $h=0$ cm are imposed on the soil surface within the infiltrometer.

Table 2 Saturated and unsaturated hydraulic properties of the soils used in the numerical simulations by SUSFEM and SWMS_2D. The unsaturated hydraulic properties of the soils are described by van GENUCHTEN model[7].

Soil layer	Upper	Lower
Saturated hydraulic conductivity K_s, m/d	0.298	0.454
Saturated soil water content θ_s	0.309	0.399
Residual soil water content θ_r	0.0001	0.0001
Coefficient in soil water retention α, cm^{-1}	1.74	1.39
Exponential in soil water retention n	1.3757	1.6024
$m=1-1/n$	0.2731	0.3759

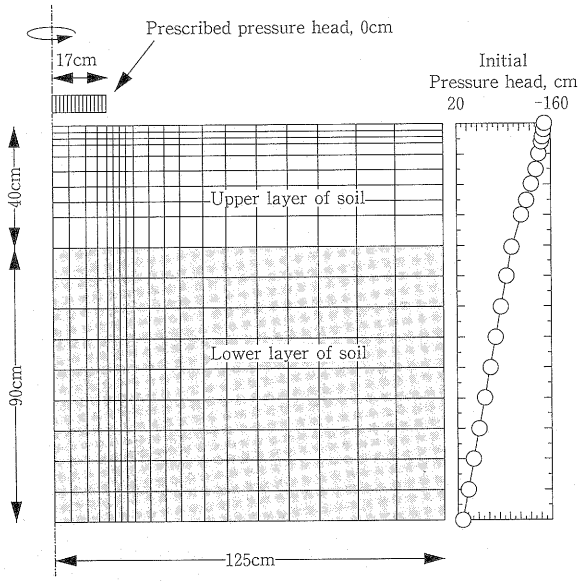

Fig. 3 Finite element mesh and initial pressure head used in the numerical simulations by SUSFEM and SWMS_2D. The soil is two-layered and radially symmetric. The constant-head infiltration is simulated over a period of 5 days.

Fig. 4 compares cumulative infiltration from the infiltrometer into soil between SUSFEM and SWMS_2D. In Fig. 5 the pressure heads are compared at $t=0.5$ and 5 days. Although there can be seen some small differences in the pressure head near an interface between two soil layers, it may be noticed that the water movements in the soils calculated by SUSFEM agree closely with those by SWMS_2D.

FIELD MEASUREMENT AND NUMERICAL ANALYSIS OF CONSTANT-HEAD INFILTRATION FROM SINGLE RING

Field measurement

The field permeability test using the pressure infiltrometer was conducted in the sand soil. Fig. 6 shows a grain distribution of the soil. The soil is classified into sand with less content of fine soil particles. A steel ring 5.5 cm in radius was inserted into the soil surface 3.0 cm in depth. The constant pressure head 9.7

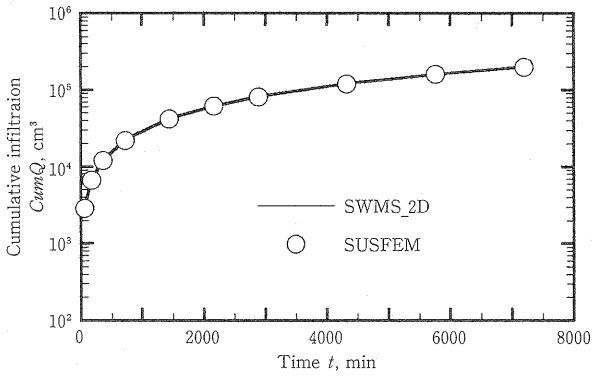

Fig. 4 Comparison of the cumulative infiltration into the soil from the infiltrometer calculated by SUSFEM with one by SWMS_2D.

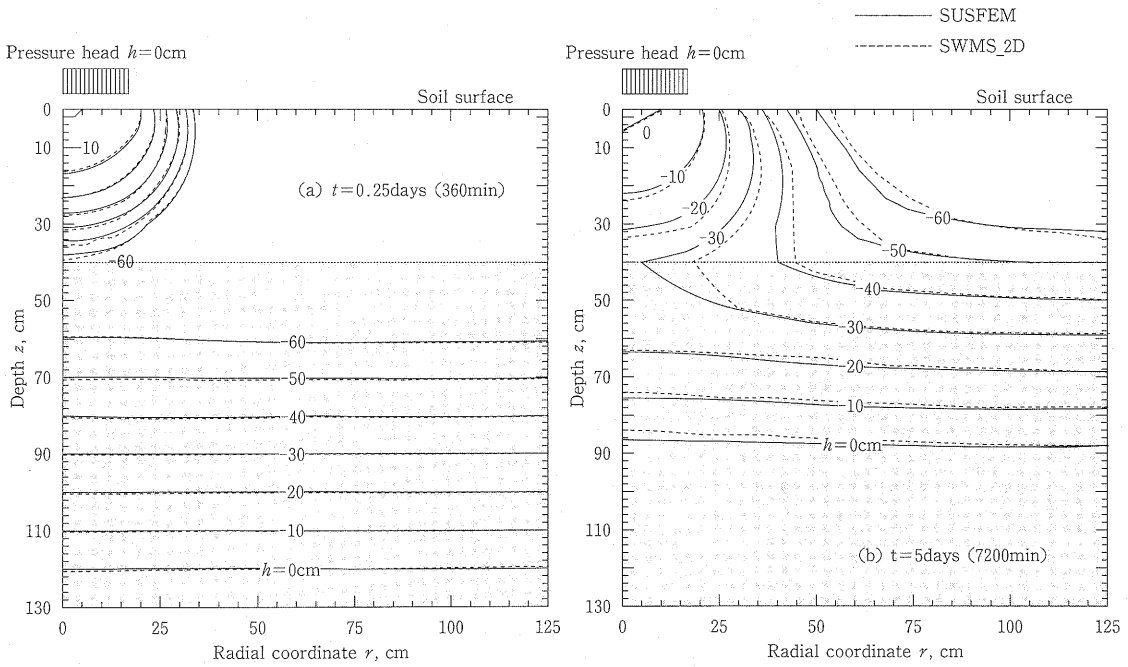

Fig. 5 Comparison of the pressure head profiles calculated by SUSFEM (solid lines) with ones by SWMS_2D (dotted lines) at the time of 0.5 and 5 days.

cm was imposed on the soil surface within the single ring during 10 minutes. The infiltration rate was measured during the constant-head infiltration from the single ring. The infiltration rate decreased soon after the beginning of the constant-head infiltration and approached to the constant value. The steady infiltration Q_s, which is calculated as an average of the infiltration rate measured during 5 to 10 minutes after the beginning of the constant-head infiltration, was 12.89 cm³/s. The pressure head and the moisture content in the soil were also monitored by four tensiometers and one moisture gauge, respectively, buried before the field permeability test as shown in Fig. 7 (a). Fig. 7 (b) shows the initial pressure head in the

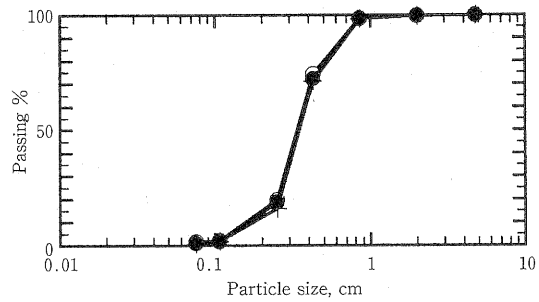

Fig. 6 Grain distribution of sand soil sampled from the test site. Three soil samples are tested.

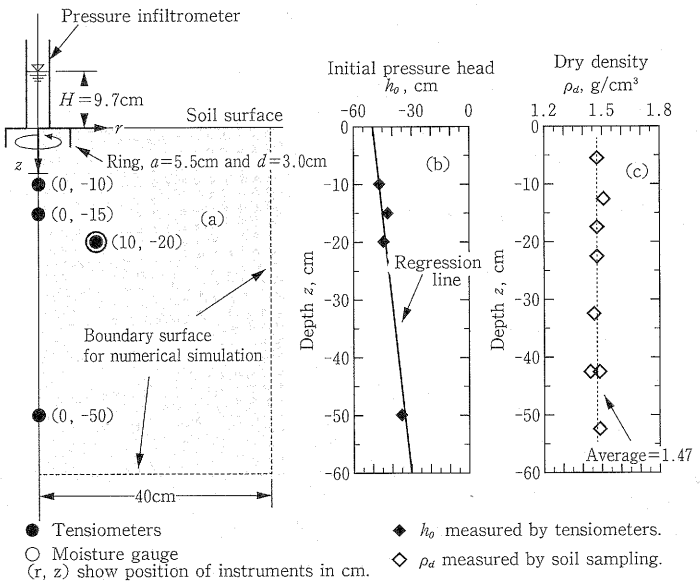

Fig. 7 Schematic diagram of the field permeability test using the pressure infiltrometer carried out in the sand soil. The soil is radially symmetric. (a) shows the measurement sensors buried in the soil together with the axisymmetric region for the numerical analysis by SUSFEM, (b) shows the initial pressure head measured in the soil and their regression line for the numerical analysis, and (c) shows the soil density profile measured by soil sampling.

soil measured before the beginning of the constant-head infiltration. After the field permeability test, 100 cc-in-volume soil cored were bored from the test site to determine the density in the soil. Fig. 7 (c) shows the soil profile uniformly compacted during burying the tensiometers and the moisture gauge.

Hydraulic properties of soil

A solid line shown in Fig. 8 is a water retention curve of the soil employed in the numerical calculation by SUSFEM. The functional shape of the water retention curve of soil is estimated on the basis of the field experiments during the drying process of water previously conducted by INOUE, et al.[8] and INOUE[9] given by a broken line and a dotted line in Fig. 8, respectively. Then the water retention curve is corrected to

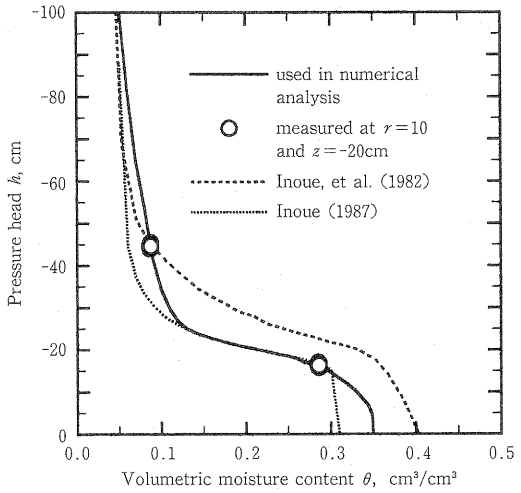

Fig. 8 Water retention curve of the sand soil. The solid line is a curve used in the numerical analysis, the broken and the dotted lines are curves during drainage process of water movement measured in the previous studies, and circles are measured in the soil before the test and during the steady infiltration from the ring.

include sets of the pressure head and the volumetric moisture content measured at $r=10$ cm and $z=-20$ cm in Fig. 7 (a). These sets of the values, denoted by circles in Fig. 8, were measured over the period of 1 minute before both the beginning and the finish of the constant-head infiltration. Saturation of the field soil is assumed to be 20 % less than the completed saturation as pointed out by CONSTANTZ, et al.[10] Assuming 2.65 of specific gravity of soil particles and noting the average value of the soil density given in Fig. 7 (c), the saturated soil water content is calculated as 0.35 cm^3/cm^3. A residual soil water content is assumed to be 0.05 cm^3/cm^3 on the basis of the previous studies shown in Fig. 8. The relative hydraulic conductivity of the sand soil is assumed to be an exponentially increasing single-valued function of a effective saturation with a exponential value of 3.5 as measured by INOUE[9]. A functional relationship between the relative hydraulic conductivity and the pressure head of the soil is given in Fig. 9.

REYNOLDS and ELRICK[2] has shown that, with measuring Q_s during the constant-head infiltration from the single ring in the field, the saturated hydraulic conductivity of soil can be determined by

$$K_{fs}=\frac{\alpha^* G Q_s}{a\alpha^* H + a + G\alpha^* \pi a^2} \tag{12}$$

$$G = 0.316 \cdot d/a + 0.184 \tag{13}$$

where a and d are the radius and the insertion depth into soil of the ring, G is a dimensionless shape factor which accounts for the geometry of the infiltration surface within the ring, and α^* is a soil parameter which simply defines the slope of ln (K_r) versus h and may be interpreted as an index of texture/structure component of soil capillarity. Since the unsaturated hydraulic conductivity or the relative hydraulic conductivity of the sand soil is not exponential function of h as shown in Fig. 9, an integrally-equivalent α^* must be determined by using a physically-based relationship between α^* and a matric flux potential as given by ELRICK and REYNOLDS[3]. Numerically integrating the K_r-h relation in Fig. 9 to calculate the matric flux potential and taking its reciprocal, the integrally-equivalent α^* is determined as 0.0683 cm^{-1}.

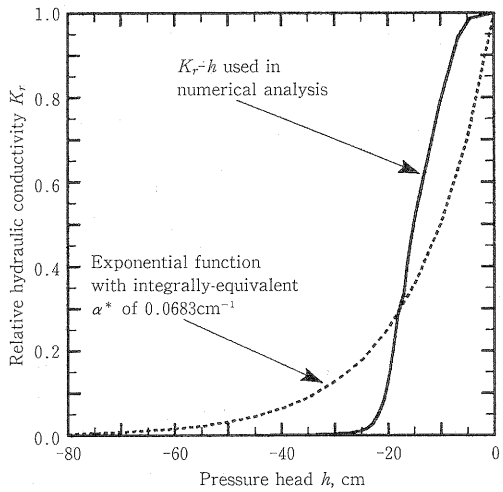

Fig. 9 Relative hydraulic conductivity of the sand soil used in the numerical analysis. The dotted line is a exponential function calculated by using the integrally-equivalent α^*.

The exponential function calculated using the integrally-equivalent α^* is given by a dotted line in Fig. 9. Inserting values of the integrally-equivalent α^* and the measured Q_s into Eq. (12) with $a=5.5$ cm and $d=3.0$ cm, then $K_s=2.738$ cm/s is obtained.

Numerical analysis

The axisymmetric water movement from the single ring into the soil is analyzed by SUSFEM. The entire region of the soil to be analyzed is 60 cm in depth and 40 cm in radius as given by the dotted lines in Fig. 7 (a). The symmetric axis, the soil surface except for within the ring, and both sides and edge of the ring inserted into the soil are considered as the impervious boundaries. 2.5 mm thickness of the steel ring is assumed. The pressure heads along the base and the vertical side of the entire region of the soil are fixed at the initial values. The pressure head in the soil at the beginning of the constant-head infiltration are distributed on the basis of a regression line of the measured pressure head shown in Fig. 7 (b). The allowable tolerance of the pressure head during the iterative calculations is set as 0.01 cm.

The infiltration rate from the ring, the pressure head and the volumetric moisture content in the soil measured with the time are compared with the calculated ones in Figs. 10 (a), 10 (b) and 10 (c), respectively. Fairly good agreements are noticed. As mentioned in the preceding section, the infiltration rate into the sand soil under the constant pressure head rapidly decreases to quasi-steady state of infiltration a few minutes after the beginning of the test. Fig. 11 shows advances of saturated water bulb and wetted zone with time calculated by SUSFEM. The saturation of the wetted zone shown in Fig. 11 is corresponding to 50 %. It is interesting to note that the size of the saturated water bulb remains almost constant after the beginning of the constant-head infiltration, whereas the wetted zone extends with the time. The size of the saturated water bulb depends on the constant pressure head imposed on the soil surface within the ring.

CONCLUSIONS

The Galerkin-type FEM is well suited for the solution of problems involving transient saturated-

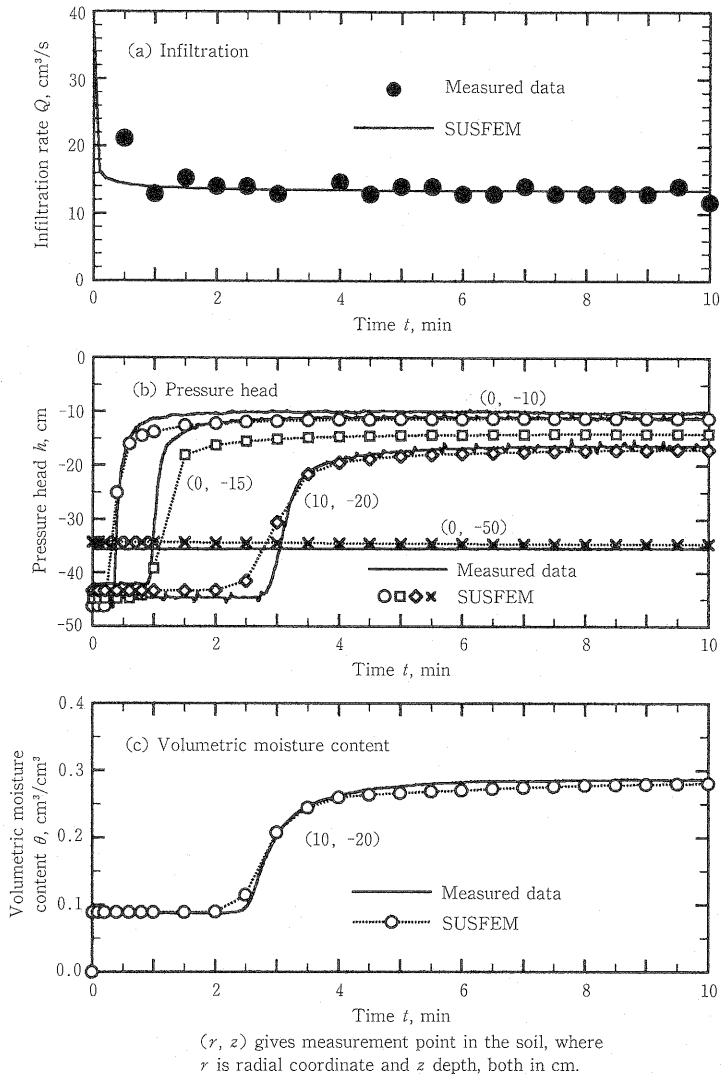

Fig. 10 Comparison of (a) infiltration rate, (b) pressure head in the soil, and (c) volumetric moisture content in the soil measured during the field permeability test with ones calculated by SUSFEM.

unsaturated water movement in soil. The Richards' potential equation supplemented by the appropriate boundary and initial conditions was formulated to develop the computer program SUSFEM for simulating the water movement in two-dimensional unsaturated, partially saturated, or saturated soil. The saturated water movement is predominant in the region where $h>0$ and the unsaturated flow in the region where $h<0$. An equi-potential line or surface corresponding to $h=0$ will be the free surface in the seepage problem, the water table in the groundwater problem, or the saturated water bulb in the infiltration problem which happens to separate the saturated and unsaturated zones in the soil. The applicability of SUSFEM was confirmed by comparing with the laboratory experiment and the computer program published in the literatures. SUSFEM was applied to analyze the constant-head infiltration from the single

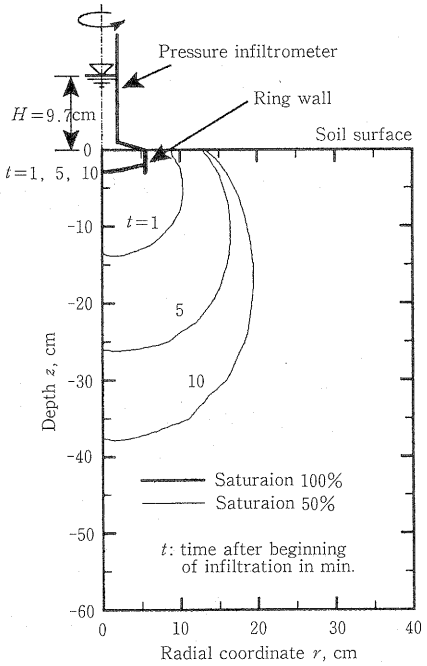

Fig. 11 Moisture movement in the soil during the constant-head infiltration calculated by SUSFEM. The saturated water bulb and the wetted zone corresponding to the saturation 50 % are given by thick and thin lines, respectively, at $t=1$, 5 and 10 minutes. Note the size of the saturated water bulb remains almost constant.

ring measured in the sand soil field. It provided good predictions of the infiltration rate into the soil as well as the water movement in the soil with employing the saturated hydraulic conductivity determined by the field permeability test.

REFERENCES

1. NEUMAN, S. P. 1973. Saturated-unsaturated seepage by finite elements. Journal of the Hydraulics Division, Proceedings of the American Society of Civil Engineers, **99**: 2233-2250.
2. REYNOLDS, W. D. and ELRICK, D. E. 1990. Ponded infiltration from a single ring: I. Analysis of steady flow. Soil Science Society of America Journal, **54**: 1233-1241.
3. ELRICK, D. E. and REYNOLDS, W. D. 1992. Infiltration from constant-head well permeameters and infiltrometers. pp. 1-24 in Topp, G. C ., Reynolds, W. D. and Green, R. E. (eds.) Advances in Measurement of Soil Physical Properties: Bringing Theory into Practice, SSSA Special Publication **30**, Soil Science Society of America, Madison, Wisconsin.
4. STEPHENS, D. B. 1996. Vadose Zone Hydrology, Lewis Publishers, PP. 135-201.
5. VAUCLIN, M., KHANJI, D. and VACHAUD, G. 1979. Experimental and numerical study of a transient, two-dimensional unsaturated-saturated water table recharge problem. Water Resources Research, **15**: 1089-1101.
6. SIMUNEK, J., VOGEL, T. and van GENUCHTEN, M. Th. 1994. The SWMS_2D code for simulating water flow and solute transport in two-dimensional variably saturated media. Research Report No. **132**, U.

S. Salinity Laboratory, Agricultural Research Service, U. S. Department of Agriculture, Riverside, California.

7. van GENUCHTEN, M. Th. 1980. A closed-form equation for predicting the hydraulic conductivity of unsaturated soils. Soil Science Society of America Journal, **44**: 892-898.
8. INOUE, M., YANO, T., YOSHIDA, I., YAMAMOTO, T. and CHIKUSHI, J. 1982. Determination of unsaturated hydraulic conductivity from soil water characteristic curve. Soil Physical Conditions and Plant Growth, Research Association of Soil Physics, National Institute of Agricultural Sciences, Japan, **46**: 21-29. (in Japanese with English summary)
9. INOUE, M. 1987. Evaluation of soil water properties during drainage periods in a sand dune field. Bulletin of the Faculty of Agriculture, Tottori University, Japan, **40**: 119-129. (in Japanese with English summary)
10. CONSTANTZ, J., HERKELRATH, W. N. and MURPHY, F. 1988. Air encapsulation during infiltration. Soil Science Society of America Journal, **52**: 10-16.

有限要素法による土壌中の水分挙動の予測

森井俊広

（平成11年5月6日受付）

摘　要

二次元または軸対称条件下の不飽和土、部分飽和土あるいは飽和土における水分挙動を予測するためのコンピュータプログラムSUSFEMを開発した。Richardsのポテンシャル方程式と初期および境界条件を説明し、Galerkin有限要素法と繰返し計算手法を用いて定式化した。SUSFEMにより、土壌中の圧力水頭hの時間的、空間的変化を計算することができる。$h>0$の領域では飽和流れが、$h<0$の領域では不飽和流れが卓越することになる。浸透流の自由水面や地下水面、浸潤流れの飽和水分球根は、$h=0$に対応する点を連ねた等ポテンシャル線として定義され、単に土壌中の飽和領域と不飽和領域とを区分するだけの物理的意味しかもたない。SUSFEMの実務性を、公表されている室内実験結果およびコンピュータプログラムとの比較により検証した。次いで、SUSFEMを、砂地ほ場で測定した単一リングからの定水頭浸潤挙動の分析に適用した。ほ場透水試験からえられた飽和透水係数を用いることにより、浸潤流量ならびに土壌中の水分挙動を良好に予測できた。

キーワード：土壌中の水分挙動、リチャードのポテンシャル方程式、有限要素法、コンピュータプログラム、ほ場透水試験